OPEN ACCESS

University of BRISTOL

Peer reviewed version

Link to published version (if available):
10.2514/6.2016-1575

Link to publication record in Explore Bristol Research
PDF-document

Doublet-Lattice Method Correction by Means of Linearised Frequency Domain Solver Analysis

C. Valente [*], D. Jones [†], A. Gaitonde [‡], J. E. Cooper[§]

Department of Aerospace Engineering, University of Bristol, Bristol, BS8 1TR, U.K.

Y. Lemmens[¶]

Siemens Industry Software NV, B-3001 Leuven, Belgium

Paper submitted as part of the special session for the ALPES Aircraft Loads Prediction Using Enhanced Simulation Project.

The main objective of this paper is to present a new methodology to correct the air loads computed with traditional potential flow models by means of linearised frequency domain analysis. The correction will be compared with the reference accurate steady and unsteady aeroelastic calculations performed with an OpenFSI methodology which strongly couples the structural solver MSC Nastran and the CFD code DLR TAU. This framework has demonstrated the capability to perform static and gust calculations for the FFAST wing, which is representative of a modern civil transport wing. An updated version of the framework will allow rigid body modes of heave and pitch to be included in the analysis. The linearised frequency domain solver has shown higher computational performance compared to unsteady time accurate simulation, hence will allow a reduction in the time necessary to compute the necessary corrections.

Nomenclature

$\mathbf{A}_{jj}$ aerodynamic influence coefficient matrix, AIC
ρ atmospheric density
$\bar{q}$ flight dynamic pressure
$\mathbf{w}_j$ downwash
$\mathbf{w}_j^g$ static aerodynamic downwash: includes initial angle of attack, camber,
       twist and gust
$\mathbf{p}_j$ pressure on lifting element j
k reduced frequency
$\mathbf{u}$ displacement and rotational degrees of freedom
$\mathbf{P}$ force vector on lifting elements $[L, M_y]$
$\mathbf{F}$ force vector on structural elements
$\mathbf{S}$ integration matrix
$\mathbf{Z}$ difference matrix
$\mathbf{D}^1$ differential matrix for deformations
$\mathbf{D}^2$ differential matrix for deformation rate
$\mathbf{\Gamma}$ circulation of panel
$\mathbf{Q}_{hh}$ Generalized Aerodynamic Forces (GAF) matrix

---

[*]Marie Curie Early Stage Research Fellow in Aircraft Loads. Email: carmine.valente@bristol.ac.uk
[†]Senior Lecturer in Aerodynamics. Email: dorian.jones@bristol.ac.uk
[‡]Senior Lecturer in Aerodynamics. Email: ann.gaitonde@bristol.ac.uk
[§]RAEng Airbus Sir George White Professor of Aerospace Engineering. Email: j.e.cooper@bristol.ac.uk
[¶]Sr. Project Leader RTD, Digital Factory Division, Product Lifecycle Management, Simulation & Test Solutions. Email: yves.lemmens@siemens.com

American Institute of Aeronautics and Astronautics

| $\mathbf{Q}_{hh}$ | generalized aerodynamic forces matrix |
| $\mathbf{Q}_{aa}$ | GAF matrix providing forces at the structural grid point due to structural deformation |

Superscripts

| nl | nonlinear quantities |

Subscripts

j	aerodynamic control point set (3/4 point of panel)
k	aerodynamic load point set (mid point on panel)
a	structural grid point set

I. Introduction

The current industrial standard for gust loads modelling is to use traditional potential flow models, such as the doublet-lattice method (DLM) and strip theory,[1,2] to generate the air loads interacting with the aircraft structure. However the growing interest in flexible-aircraft dynamics has highlighted how these models make simplifying assumptions that may not allow an accurate prediction of the air loads in these cases. Since linear unsteady aerodynamics show inaccuracies in the transonic regime, where the linear assumptions are no longer valid and the effects of viscosity and thickness are relevant, many correction techniques have been developed in the past years[3,4] to attempt to address this issue. Their aim is to introduce wind tunnel data and Computational Fluid Dynamics (CFD) results into the linear unsteady aerodynamics[5,6] to give improved predictions in this flight regime. Unfortunately most of them rely on a large quantity of additional data. The increased availability of high performance computing, has seen the development of reliable fluid and structural solvers for use in the engineering design process.[7–9] In the aeroelastic domain, fluid structure interaction procedures are always more often considered as a means to replace expensive experimental campaigns.

A new Open Fluid Structure Interaction (OpenFSI) has been developed to strongly couple the structural finite element (FE) code MSC Nastran and the CFD code DLR TAU.

The developed interface is available in the solution sequence SOL 400 of MSC Nastran, and can be used to compute both steady or unsteady aeroelastic calculations. Preliminary results have been compute using the FFAST right wing model,[10] a representative model of a general single aisle civil aircraft. The capability to investigate steady aeroelastic problems has been first demonstrated through aeroelastic convergence of trim calculations, before an application for a gust load investigation could be carried out.

The work presented in this paper aims to present a new approach to correct the air loads computed using DLM, by means of linearised frequency domain solver analysis.
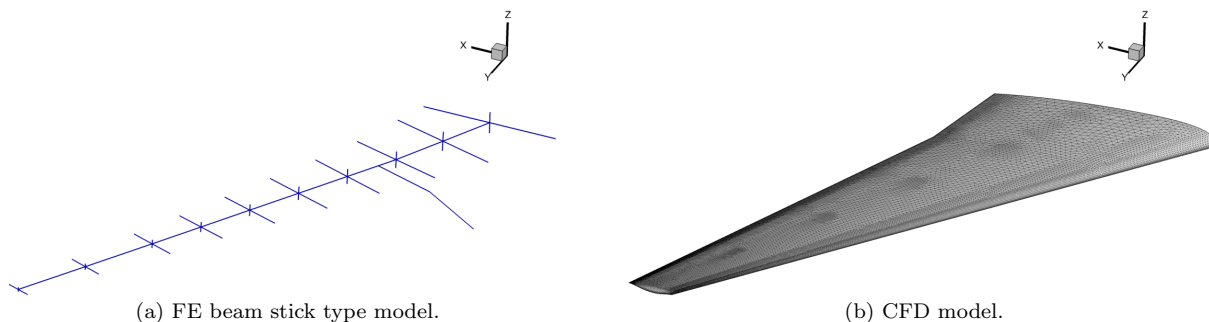

(a) FE beam stick type model.

(b) CFD model.

Figure 1: FFAST right wing model.

II.   Aeroelastic Model

A full aircraft model was developed as part of the FFAST project[10] to be representative of a single-aisle civil jet airliner. The structural model of the aircraft is a beam stick FE model with lumped masses. In this paper aeroelastic analysis have been computed using the FFAST right wing considered clamped at the root, for the FEM, and a CFD model has been created in order to match the jig shape of the structure. The wing CFD model (created using aerofoil data available for the three sections: root, crank and tip) does not include the engine and pylon, and has 33227 surface grid points. The FE model contains 10 beam elements for a total of 11 structural grid points. A comparison of the two models is shown in Figure 1.

A.   Strongly coupled Gust analysis using the ALPESOpenFSI Interface

The need for an high fidelity analysis environment, able to compute steady and unsteady aeroelastic computation, has driven to the definition of a new Open Fluid Structure Interface (OpenFSI), called ALPESOpenFSI. This interface developed making use of the MSC Nastran Application Program Interface (API), provides a mean to generate an interface between the Finite Element Code and an external Computational Fluid Dynamic Solver(CFD). In the specific case the CFD code chosen has been the DLR TAU-code. The ALPE-SOpenFSI interface is available within the Nonlinear Static and Transient Solution, inside the framework of the nonlinear solution sequence MSC Natran SOL400.
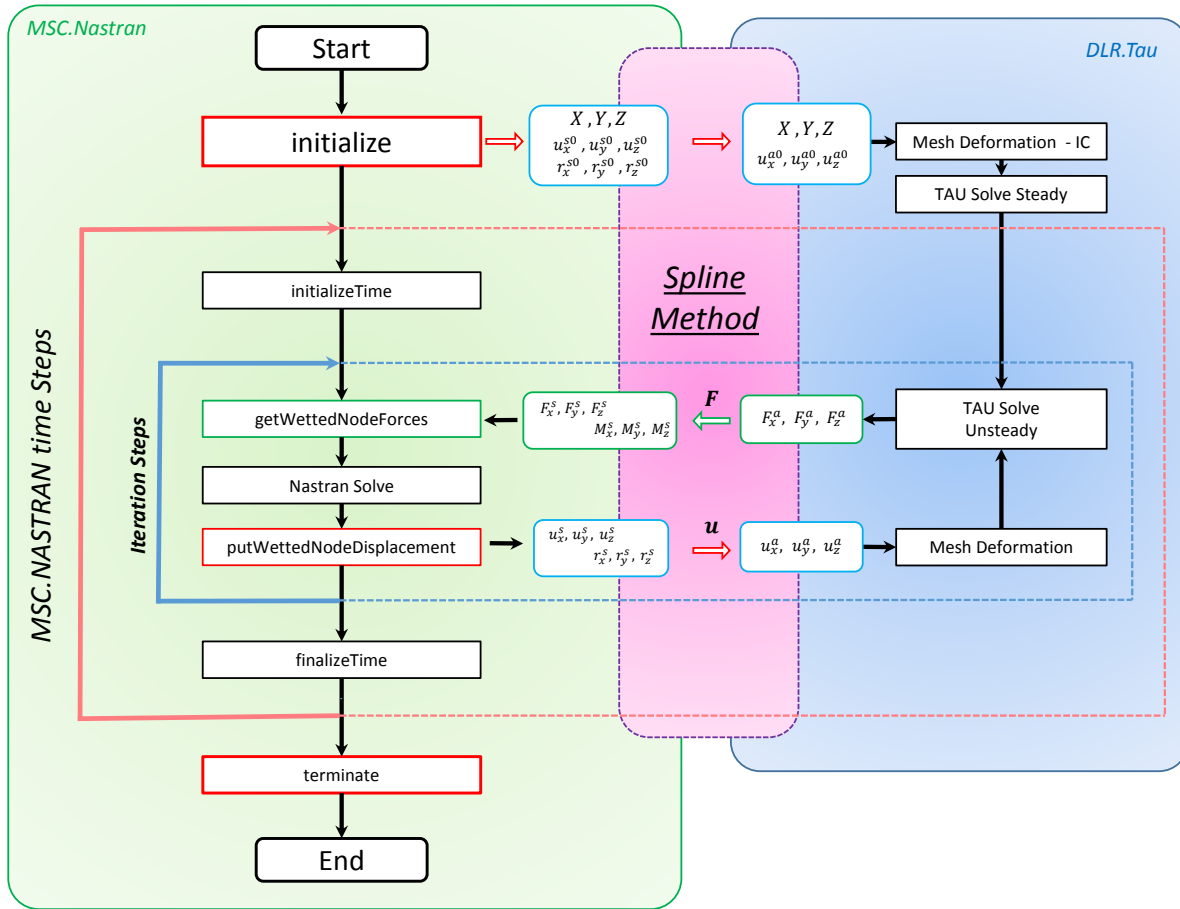

Figure 2: ALPESOpenFSI interface for coupled FEM/CFD simulations.

The OpenFSI interface manages the exchange of information between the FEM and CFD code, which execute simultaneously during a coupled analysis. The control on the analysis sequence is managed by MSC Nastran, which initialize the simulation, and after on the base of the nodal forces computed from the external code, computes the structural displacement, velocity and acceleration. These information are then necessary

American Institute of Aeronautics and Astronautics

to update the CFD mesh. The mentioned quantities are exchanged on the so called "wetted nodes", a set of the structural grids, sensible lower of the node characteristic of the CFD surface mesh. For this reason it is required to adopt an adequate spline methods to ensure the accurate transfer of the these quantities.

In the implementation of the interface two methodologies have been used to obtain the interpolation matrix. The first based on radial basis funciton method by Rendall and Allen.[11,12] The second based on the 3D beam and 3D surface available in MSC Nastran using SPLINE6 and SPLINE7.[13]

In a loosely coupled approach, the flow an the structural solver are out of sync. A strongly coupled approach has been chosen to avoid the first order error associated with the time-step. To realize a strongly coupled analysis the stream management in TAU has been modified, and a variable initialization from two different streams has been realized.

An overiview of the "ALPESOpenFSI" interface is given in Figure (2)

Using the same interface is possible to compute static aeroelastic analysis, trough the Non Linear Static (NLSTAT) analysis or investigate the unsteady response of the structure to a gust disturbance, with the Non Linear Transient (NLTRAN) analysis, or the two can be combined.

To validate the interface the flutter behavior of the AGARD 445.6 wing has been studied in.[14]

B.   Non linear static analysis for aeroelastic trim

As part of the FFAST project,[10] a full aircraft model was developed, in order to have a representative model of a single-aisle civil jet airliner. The ALPESOpenFSI interface been used to study the aerolastic trim deformation and the gust response of the FFAST right wing model.

The flight condition used in the investigation is a $1g$ condition at 11000 m, Mach number $M = 0.85$ and $2°$ angle of attack. The CFD model has been solved using Euler equations. The wing CFD mesh does not include the engine and pylon and has 33227 surface grid points. The structural model is a beam stick model with lumped masses, characterized by 10 beam elements for a total of 11 structural grid points. Figure 1 shows a comparison of the two models. The trim analysis has allow to identify the elastic static deformation of the wing, and the convergence to a wing tip vertical displacement of 7.01 cm is shown in Figure 3.

(a) Wing tip node vertical displacement.
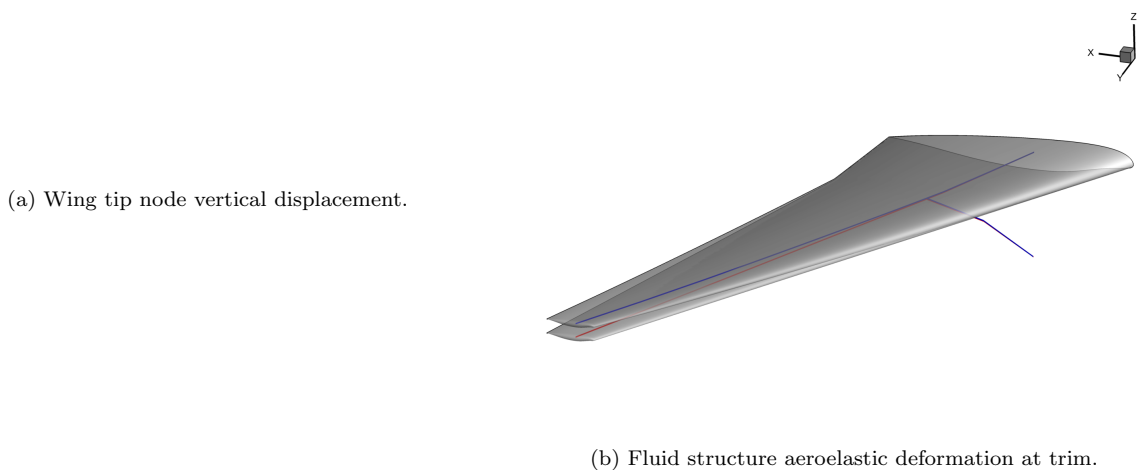

(b) Fluid structure aeroelastic deformation at trim.

Figure 3: FFAST wing trim analysis.

From this initial condition a transient analysis has been performed to compute the gust loads which the structure is subject. The gust is modelled in TAU, using a field velocity method.[15–17] It is prescribed to start just outside the computational domain and travel at free stream velocity U_∞. In the following example a value of F_g equal to 1 has been considered.

C. Unsteady transient analysis for gust

Figure 4 shows a typical one minus cosine (1MC) gust velocity profile, having a maximum gust velocity of w_{g0} and gust wavelength of L_g. As prescribed by the "Certification Specification for Large Aeroplanes CS-25",[18] the shape of the gust has to be taken as:

$$v_g(x) = \begin{cases} \dfrac{U_{ds}}{2}\left(1 - \cos\left(\dfrac{\pi x}{H}\right)\right) & for \;\; 0 \leq x \leq 2H \\[2em] 0 & otherwise \end{cases} \tag{1}$$

where x is the distance penetrated into the gust, U_{ds} is the design gust velocity in equivalent air speed (EAS), defined by eq. (2), and H (in m) is the distance parallel to the flight path of the aeroplane for the gust to reach its peak velocity ($H = L_g/2$, half of the gust wavelength). The design gust velocity is then defined as:

$$U_{ds} = U_{ref} F_g \left(\frac{H}{106.68}\right)^{1/6} \tag{2}$$

where U_{ref} is the reference gust velocity in EAS and F_g is the flight profile alleviation factor. U_{ref} reduces linearly from 17.07 m/s EAS at sea level to 13.41 m/s EAS at 4572 m (15000 ft) and then again to 6.36 m/s EAS at 18288 m (60000 ft).

(a) $1 - \cos$ gust shape[19]
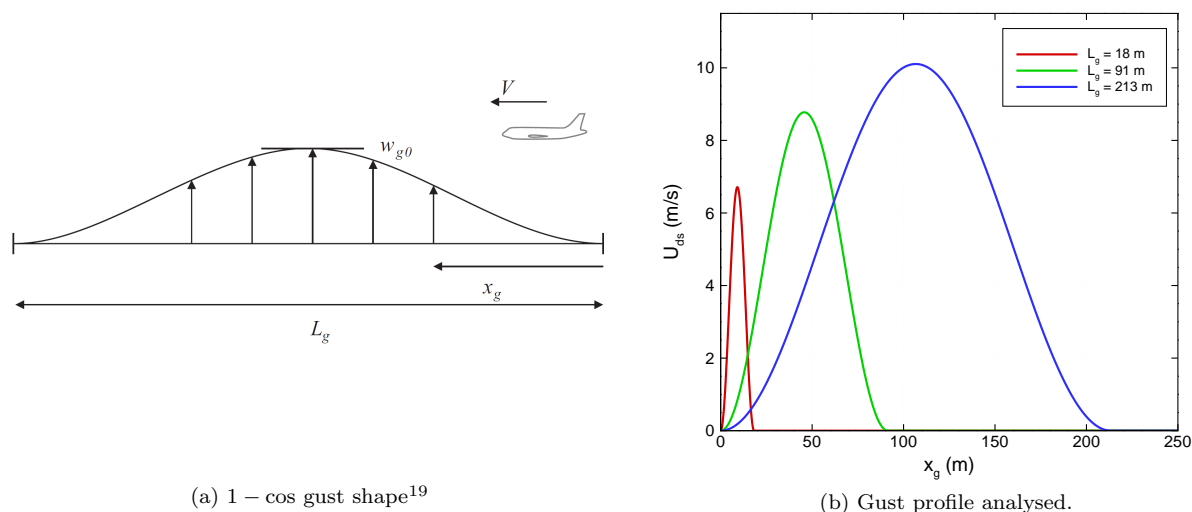

(b) Gust profile analysed.

Figure 4: Gust profile.

In the following example a value of F_g equal to 1 has been considered. Three reference gust length have been analysed and their shapes are depicted in Figure 4.

Figure 5 shows the time history of the variation of the global lift and pitching moment coefficient due to the three gust lengths.

The loads at the wing root computed by the structural solver, are presented in Figure 6.

D. Comparing DLM and Strongly coupled results

One of the standard methods to compute the loads dues to a gust is to make use of the commercial solution SOL146 from MSC Nastran. In order to evaluate the difference in the loads estimation using the fully coupled environment or the linear panel method, a comparison is shown in Figure (7).

(a) Total wing C_L.
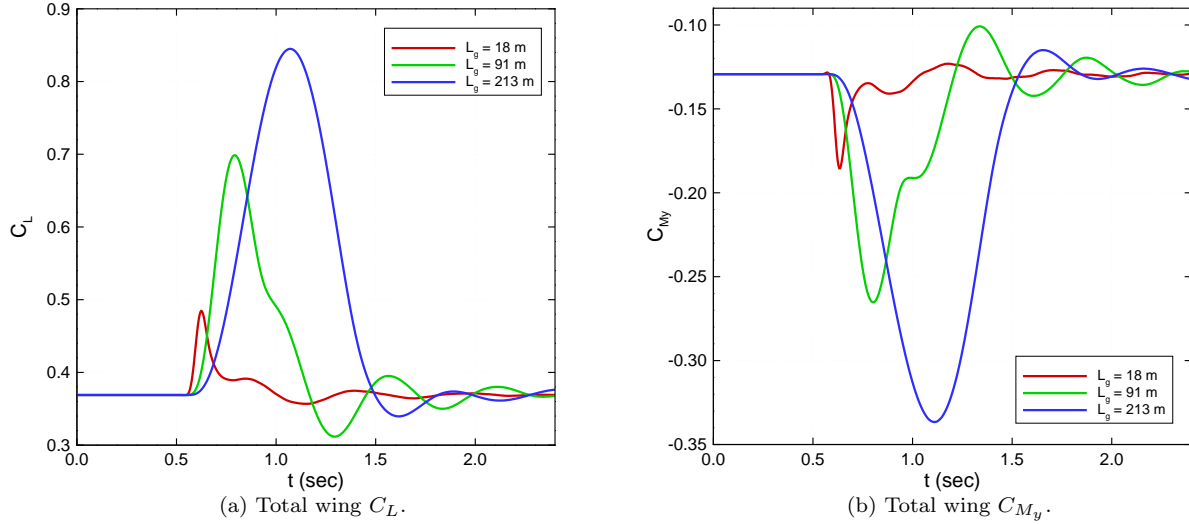

(b) Total wing C_{M_y}.

Figure 5: CFD results due to the gust.

In order to reduce the produce a more accurate loads estimation using the DLM, a first correction has to be performed in order to include the effect of camber and thickness in the calculation of the static loads. While in the full coupled analysis the effects of the initial angle of attack and aerodynamic shape are considered in the computation, in the linear approach the static aeroelastic loads have to computed and added to the gust response analysis which is computed starting form an initial angle of attack of 0 deg.

III.   DLM Correction to match Structural Loads

A.   Strip approach to compute CFD integrated Laods

In this subsection I will give a view on how the integrated loads are computed, with a couple of picture showing the slice on the cfd mesh, and plotting the integrated loads for the different CFD mesh

IV.   Post-multiply single mode for Static Trim Correction

The aim of the structural integrated load matching downwash correction method is to use steady and unsteady non linear loads obtained from CFD analysis to compute the correction matrix that is applied to the downwash. The post multiplying approach is preferable in order to avoid numerical problem due to the pressure distribution. It is possible to define and experimental downwash given by

$$\mathbf{w}^{exp} = \mathbf{W}_w \mathbf{w}^{th} \tag{3}$$

where $\mathbf{W}_w$ is the downwash correction matrix. In this specific case the experimental results are replaced with non linear CFD computation, while the theoretical results are the ones obtained from the DLM. So this relation can be rewritten as:

$$\mathbf{w}^{CFD} = \mathbf{W}_w \mathbf{w}^{DLM} \tag{4}$$

The estimate of the high fidelity pressure distribution becomes:

$$\Delta \mathbf{C}_p^{CFD} = \mathbf{A}^{-1} \, \mathbf{w}^{CFD} \tag{5}$$

so

$$\Delta \mathbf{C}_p^{CFD} = \mathbf{A}^{-1} \, \mathbf{W}_w \mathbf{w}^{DLM} \tag{6}$$

Alternatively the integrated loads can be matched instead of trying to match the pressure data, and in term of integrated aerodynamic loads

$$\mathbf{P}_k^{CFD} = \bar{q} \mathbf{S} \mathbf{A}^{-1} \, \mathbf{W}_w \mathbf{w}^{DLM} \tag{7}$$

American Institute of Aeronautics and Astronautics

(a) Wing tip vertical displacement.

(b) Total F_z at root.

(c) M_x moment at root.
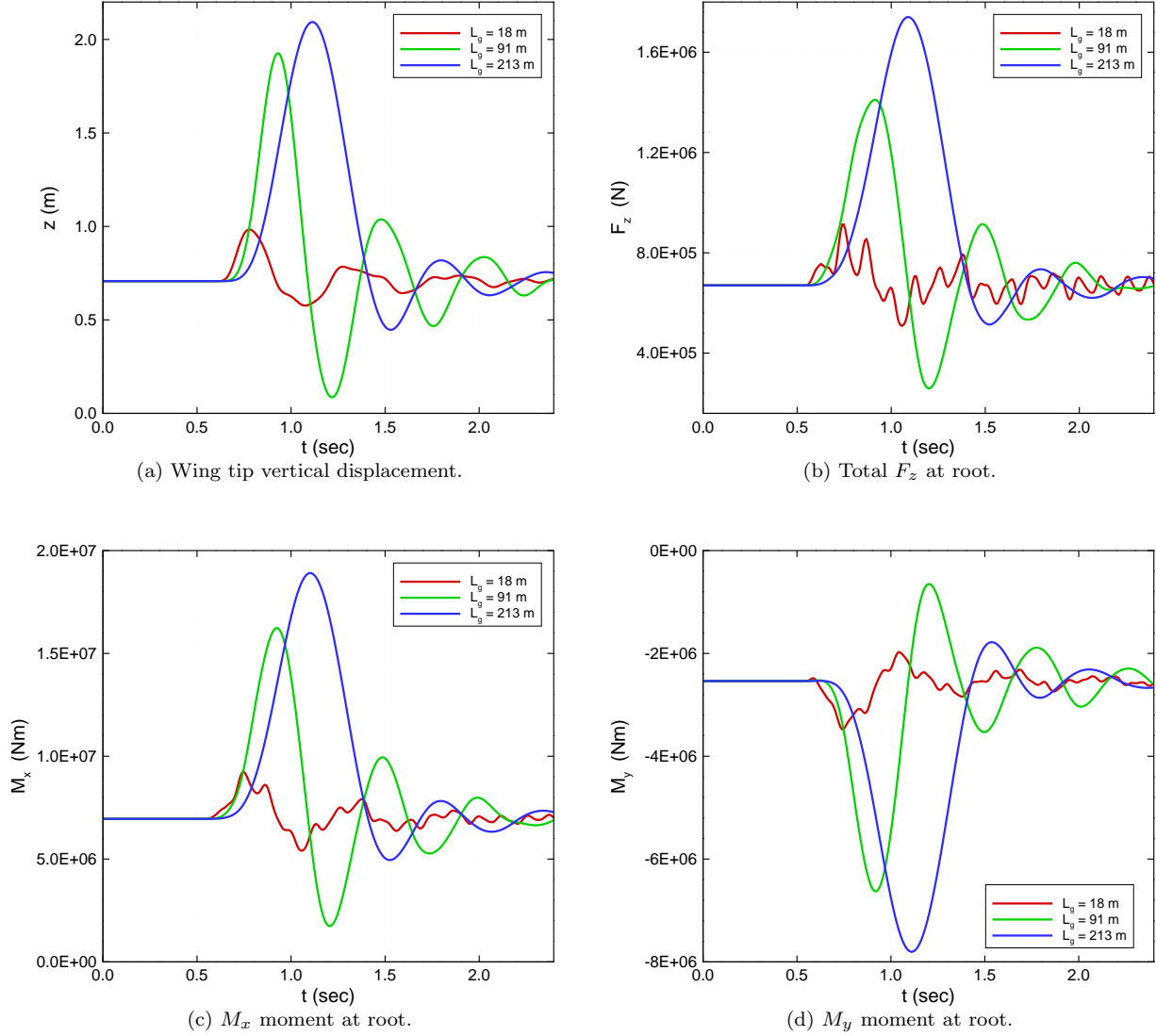

(d) M_y moment at root.

Figure 6: FE model loads resultant at wing root.

Figure 7: Comparison of the gust loads computed with the DLM or OpenFSI.(!!! PICTURE TO BE INCLUDED !!!)

Is is then possible to add an additional therm that account for the forces due to the α_0 CFD contribution

$$\mathbf{P}_k^{CFD} = \bar{q}\mathbf{S}\mathbf{A}^{-1}\ \mathbf{W}_w\mathbf{w}^{DLM} + \bar{q}\mathbf{S}_{kj}\mathbf{F}_j^e \qquad (8)$$

And in therms of aerodynamic loads applied on the structural nodes:

$$\mathbf{F}_a^{CFD} = \bar{q}\mathbf{G}_{ka}^T\mathbf{S}_{kj}\mathbf{A}_{jj}^{-1}\ \mathbf{W}_{jj}^w\mathbf{w}_j^{DLM} + \bar{q}\mathbf{G}_{ka}^T\mathbf{S}_{kj}\mathbf{F}_j^e \qquad (9)$$

To be able to solve this problem the correction process aims to find the matrix $\mathbf{W}_{jj}^w$ such that the theoretical sectional loads computed with the DLM F_a^{DLM} match the reference loads computed with the CFD, F_a^{CFD}. This problem has more solution than unknown so it leads to an undetermined system to solve
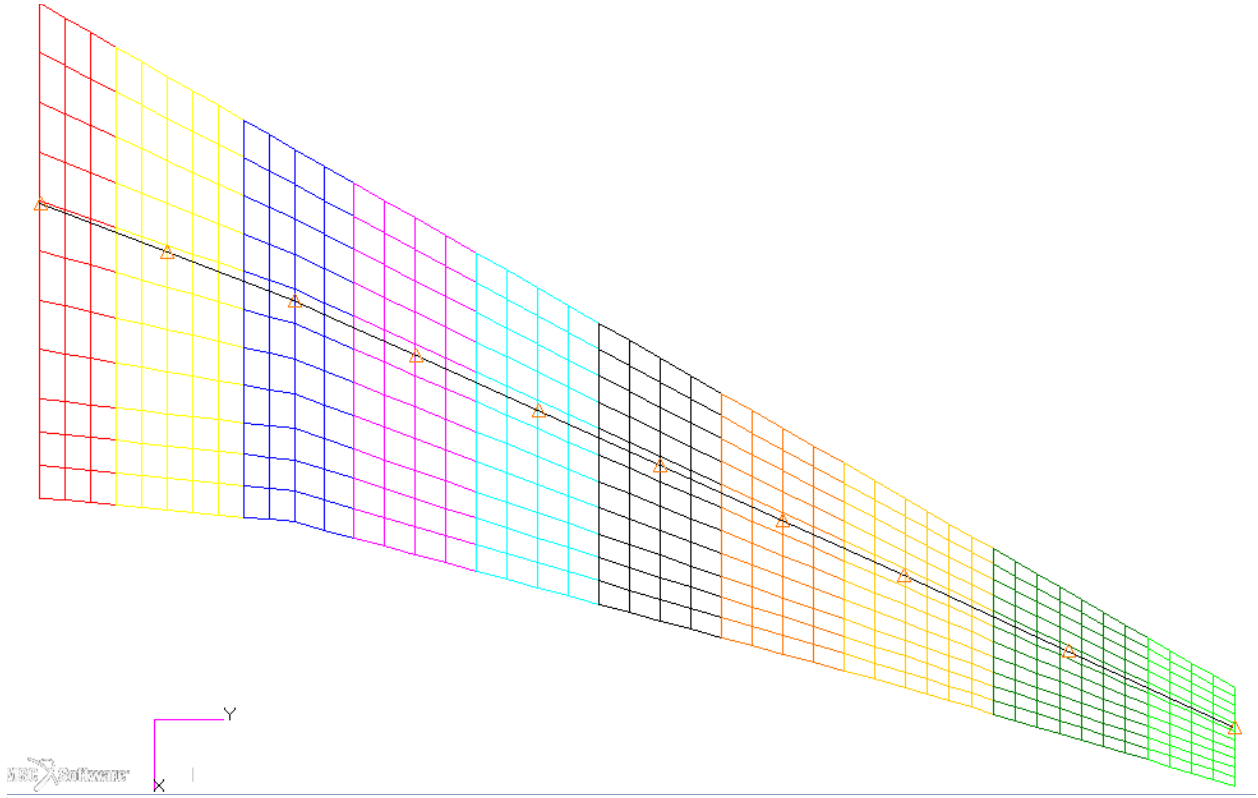
American Institute of Aeronautics and Astronautics

Figure 8: DLM Strips

for $\mathbf{W}_{jj}^w$. The requirement is tha thte change sin the theoretical loads distribution shall be a s small as possible. This mean minimising the weighted sum of the square of the deviaitons, where the deviation $\mathbf{W}_{jj}^w$ is defined as the difference between the correction factor and the unity

$$\mathbf{W}_w = \mathbf{I} + \epsilon^w \tag{10}$$

This leads to a set of equations:

$$\mathbf{F}_a^{CFD} = \bar{q}\mathbf{G}^T\mathbf{S}\mathbf{A}^{-1}\lceil\mathbf{I} + \epsilon^w\rfloor\mathbf{w}^{DLM} + \bar{q}\mathbf{G}_{ka}^T\mathbf{S}_{kj}\mathbf{F}_j^e \tag{11}$$

$$\mathbf{F}_a^{CFD} = \bar{q}\mathbf{G}^T\mathbf{S}\mathbf{A}^{-1}\mathbf{w}^{DLM} + \bar{q}\mathbf{G}^T\mathbf{S}\mathbf{A}^{-1}\epsilon^w\mathbf{w}^{DLM} + \bar{q}\mathbf{G}_{ka}^T\mathbf{S}_{kj}\mathbf{F}_j^e \tag{12}$$

$$\mathbf{F}_a^{DLM} = \bar{q}\mathbf{G}^T\mathbf{S}\mathbf{A}^{-1}\mathbf{w}^{DLM} \tag{13}$$

$$\mathbf{\Delta F}_a = \mathbf{F}_a^{CFD} - \mathbf{F}_a^{DLM} \tag{14}$$

$$\mathbf{\Delta F}_a = \bar{q}\mathbf{G}^T\mathbf{S}\mathbf{A}^{-1}\epsilon^w\mathbf{w}^{DLM} + \bar{q}\mathbf{G}_{ka}^T\mathbf{S}_{kj}\mathbf{F}_j^e \tag{15}$$

From this equation the left hand side term is known, as well as $\mathbf{S}$, $\mathbf{G}$, $\mathbf{A}$ and $\mathbf{w}$ are known from the aerodynamic model. This undetermined problem can be solved using a least squares approach.

For a static Trim analysis the DLM computes two contributions:

$$\mathbf{F}_a^{DLM} = \bar{q}\mathbf{G}_{ka}^T\mathbf{S}_{kj}\mathbf{A}_{jj}^{-1}\mathbf{D}_{jk}\mathbf{G}_{ka}\mathbf{u}_a + \bar{q}\mathbf{G}_{ka}^T\mathbf{S}_{kj}\mathbf{A}_{jj}^{-1}\mathbf{D}_{jx}\mathbf{u}_x \tag{16}$$

The first term at the right hand side is due to the presence of the structural deformation, while the second is related to the presence of the unity displacement of the aeroelastic extra point.

Considering the case of a rigid aerodynamic this equation become:

$$\mathbf{F}_a^{DLM} = \bar{q}\mathbf{G}_{ka}^T\mathbf{S}_{kj}\mathbf{A}_{jj}^{-1}\mathbf{D}_{jx}\mathbf{u}_x \tag{17}$$
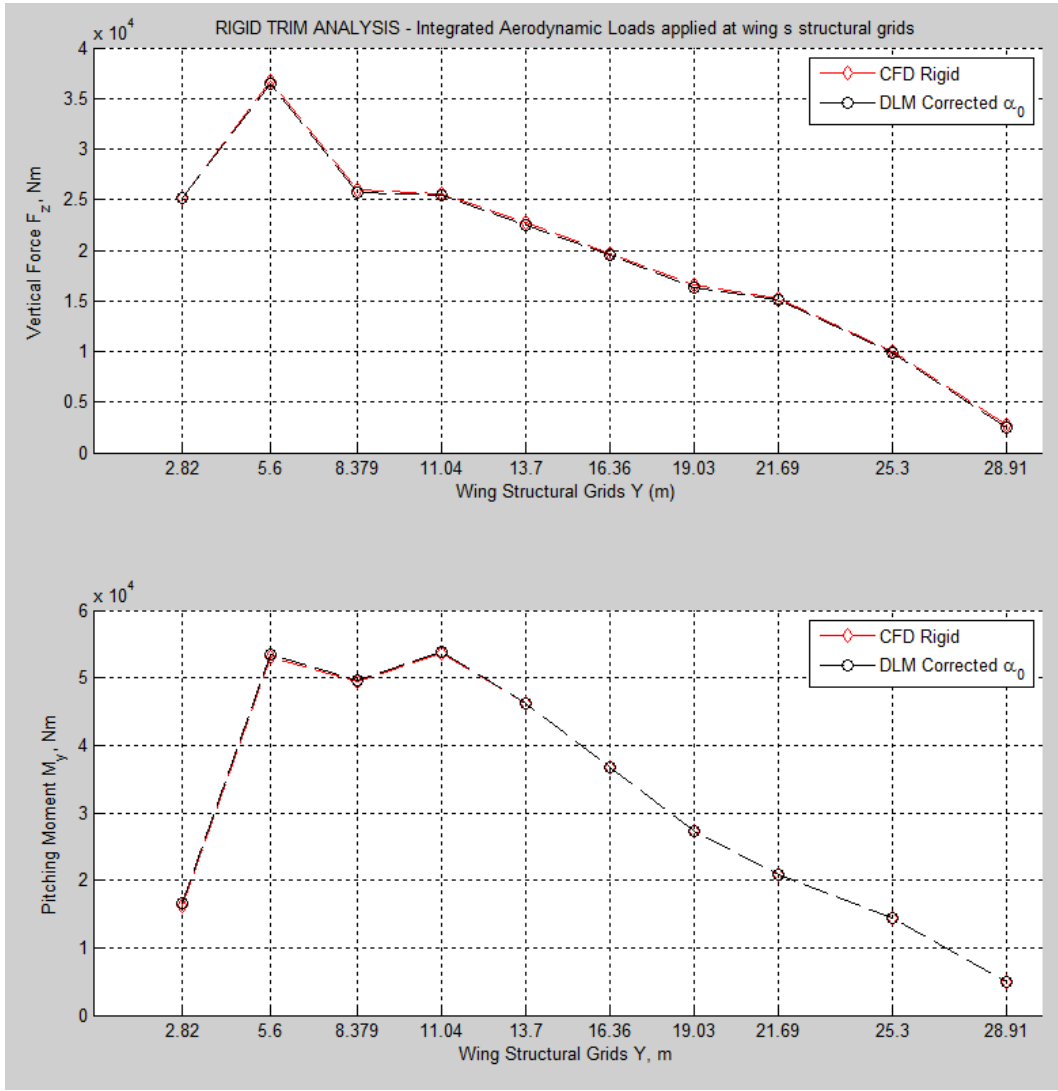
Figure 9: Corrected DLM to match the structural load at $AoA = 0$.

and in the case of a wing clamped at root, without control surface the only variable remain the angle of attach

$$\mathbf{u}_x = \{\alpha\} \tag{18}$$

If we want to compare the results that come from two CFD analysis for two different angle of attack, the system has to be modified in:

To calculate the two unknowns, Equation (15) has to be specialized for two reference case, that in this case are the 0 *deg* condition and the reference angle of attack at which the loads want to be computed, for example 2 *deg*.

$$\mathbf{\Delta F}_a^1 = \bar{q}\mathbf{G}^T\mathbf{S}\mathbf{A}^{-1}\epsilon^w\mathbf{D}_{jx}\mathbf{u}_x^1 + \bar{q}\mathbf{G}_{ka}^T\mathbf{S}_{kj}\mathbf{F}_j^e \tag{19}$$

$$\mathbf{\Delta F}_a^2 = \bar{q}\mathbf{G}^T\mathbf{S}\mathbf{A}^{-1}\epsilon^w\mathbf{D}_{jx}\mathbf{u}_x^2 + \bar{q}\mathbf{G}_{ka}^T\mathbf{S}_{kj}\mathbf{F}_j^e \tag{20}$$

$$\begin{Bmatrix} \mathbf{\Delta F}_a^1 \\ \mathbf{\Delta F}_a^2 \end{Bmatrix} = \begin{Bmatrix} \bar{q}\mathbf{G}_{ka}^T\mathbf{S}_{kj}\mathbf{A}_{jj}^{-1}\mathbf{D}_{jx}\mathbf{u}_x^1 & \bar{q}\mathbf{G}_{ka}^T\mathbf{S}_{kj} \\ \bar{q}\mathbf{G}_{ka}^T\mathbf{S}_{kj}\mathbf{A}_{jj}^{-1}\mathbf{D}_{jx}\mathbf{u}_x^2 & \bar{q}\mathbf{G}_{ka}^T\mathbf{S}_{kj} \end{Bmatrix} \begin{Bmatrix} \epsilon^w \\ \mathbf{F}_j^e \end{Bmatrix} \tag{21}$$
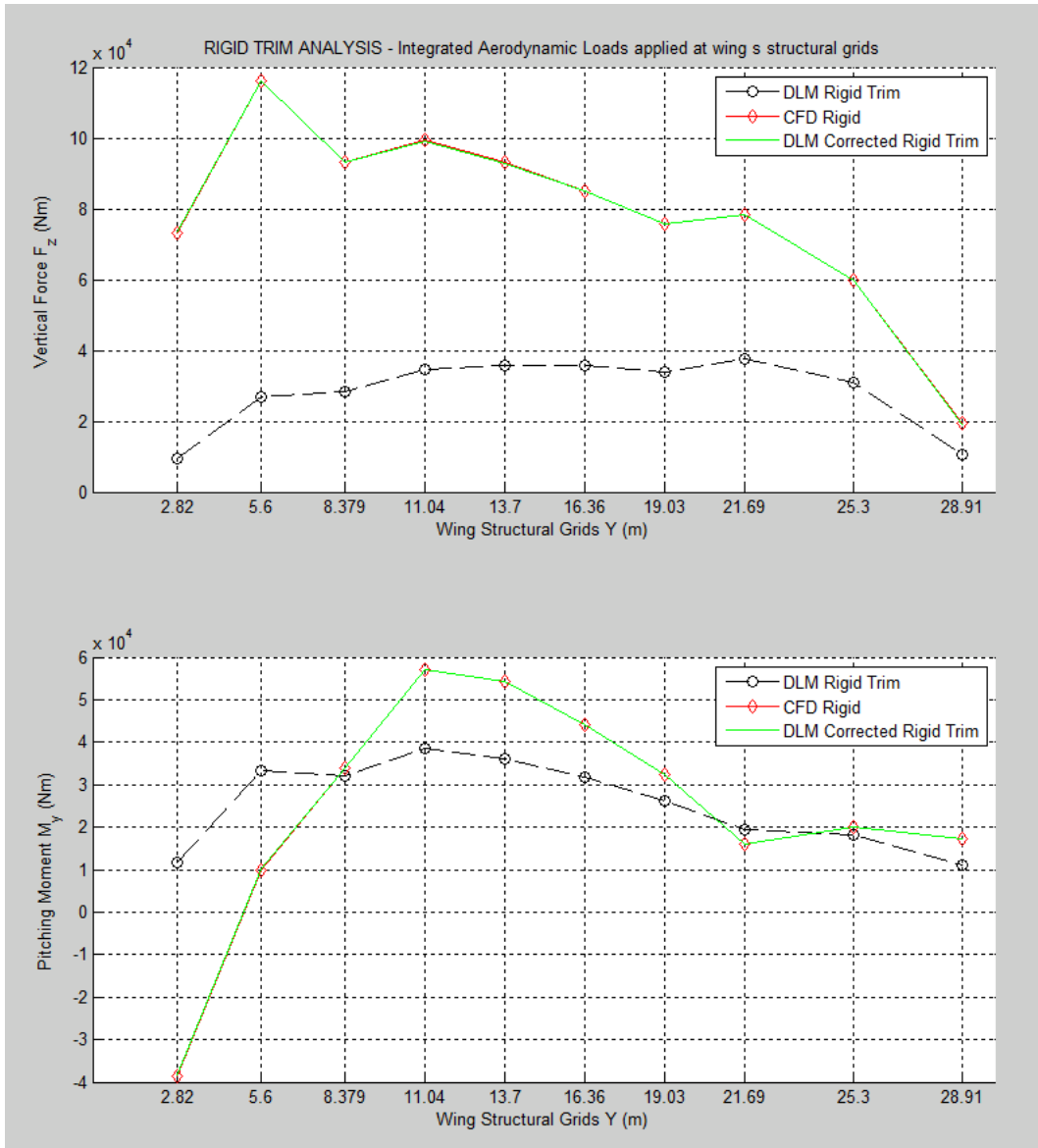
American Institute of Aeronautics and Astronautics

Figure 10: Rigid Trim Analysis - Correction computed on Rigid CFD.

A this point the corrected rigid aerodynamic forces are given by:

$$\hat{\mathbf{F}}_{a_R}^{DLM} = \bar{q}\mathbf{G}_{ka}^T\mathbf{S}_{kj}\mathbf{A}_{jj}^{-1}\mathbf{W}_{jj}^w\mathbf{D}_{jx}\mathbf{u}_x + \bar{q}\mathbf{G}_{ka}^T\mathbf{S}_{kj}\mathbf{F}_j^e \tag{22}$$

Using the same correction matrix even for the elastic contribution, it possible to express the forces to the structural displacement as:

$$\hat{\mathbf{F}}_{a_E}^{DLM} = \bar{q}\mathbf{G}_{ka}^T\mathbf{S}_{kj}\mathbf{A}_{jj}^{-1}\mathbf{W}_{jj}^w\mathbf{D}_{jk}\mathbf{G}_{ka}\mathbf{u}_a \tag{23}$$

At this point the loads due to the rigid and elastic contribution can be estimated, and them allow to evaluate the total forces applied on the structure and reported in the following pictures

$$\hat{\mathbf{F}}_{a_{Total}}^{DLM} = \bar{q}\mathbf{G}_{ka}^T\mathbf{S}_{kj}\mathbf{A}_{jj}^{-1}\mathbf{W}_{jj}^w\mathbf{D}_{jk}\mathbf{G}_{ka}\mathbf{u}_a + \bar{q}\mathbf{G}_{ka}^T\mathbf{S}_{kj}\mathbf{A}_{jj}^{-1}\mathbf{W}_{jj}^w\mathbf{D}_{jx}\mathbf{u}_x + \bar{q}\mathbf{G}_{ka}^T\mathbf{S}_{kj}\mathbf{F}_j^e \tag{24}$$

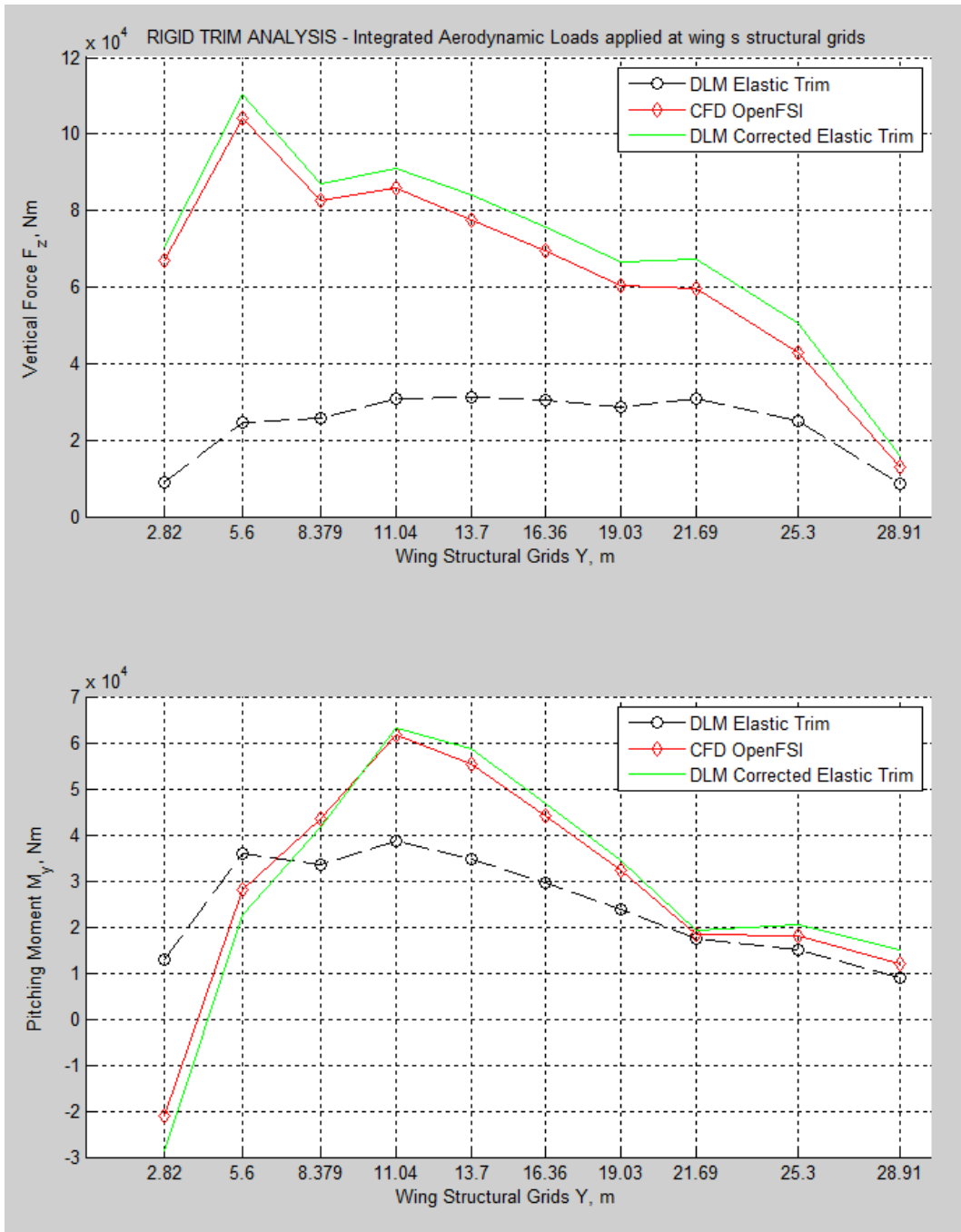American Institute of Aeronautics and Astronautics

Figure 11: Elastic Trim Analysis - Correction computed on Rigid CFD.

V. Post-multiply single mode for Gust Analysis

The generalized aerodynamic forces due to motion can be written as:

$$\mathbf{Q}^a = \bar{q}\ \mathbf{Q}_{hh}(M, k)\ \mathbf{u}_h \qquad (25)$$

while the generalized aerodynamic loads due to the aerodynamic gust can be instead written as:

$$\mathbf{Q}^e = \bar{q}w_g\mathbf{PP}(\omega)\mathbf{Q}_{hj}(M, k)\mathbf{w}_j(\omega) \qquad (26)$$
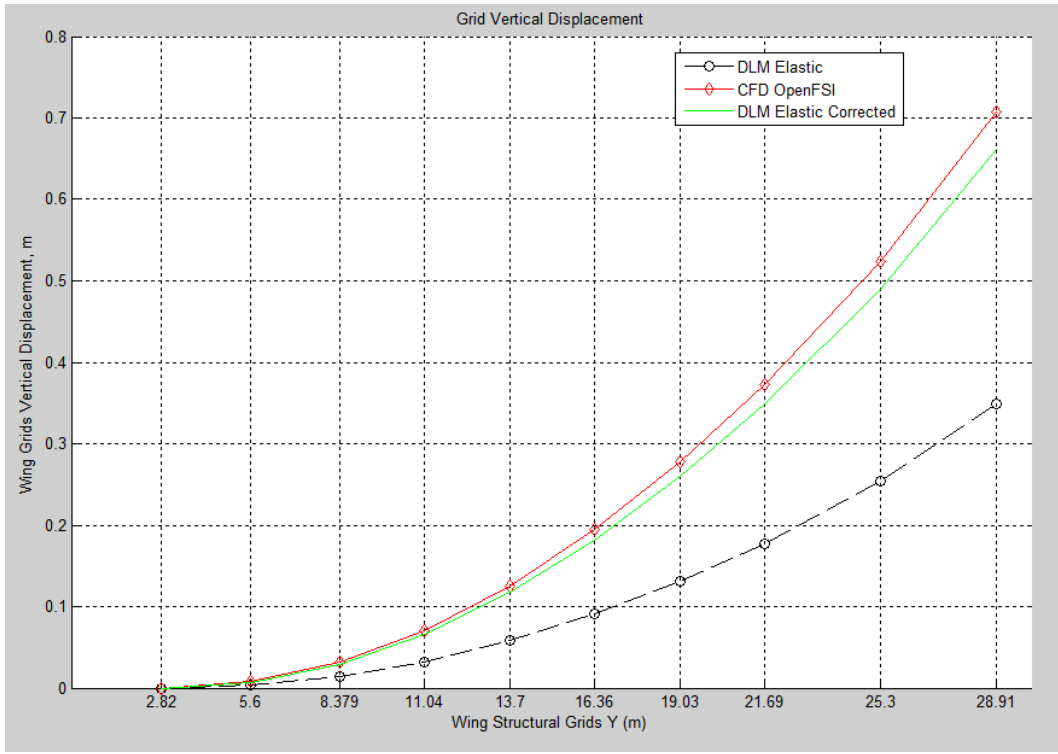
where:

Figure 12: Wing Structural Grid Vertical Displacement

w_g gust scalar factor

$\mathbf{PP}(\omega)$ user-supplied frequency variation of the gust, it can be obtained from a Fourier transform of the user-supplied discrete gust

$\mathbf{Q}_{hj}$ matrix supplying the generalized aerodynamic forces (in the modal h-set) due to the downwash vector

$\mathbf{w}_j(\omega)$ downwash vector applied at the collocation points.

From Eqs. (29) and (35) the governing equation assumes the form:

$$\left[-\omega^2 \mathbf{M}_{hh} + i\omega \mathbf{B}_{hh} + (1+ig)\,\mathbf{K}_{hh} - \bar{q}\mathbf{Q}_{hh}(M,k)\right]\mathbf{u}_h = \bar{q}w_g\mathbf{PP}(\omega)\mathbf{Q}_{hj}(M,k)\mathbf{w}_j \tag{27}$$

Considering a modal reduction, the matrix can be expressed in the generalized form:

$$\mathbf{Q}_{hh}(M,k) = \phi_{ai}^T \mathbf{G}_{ka}^T \mathbf{S}_{kj} \mathbf{A}_{jj}^{-1} \mathbf{D}_{jk} \mathbf{G}_{ka} \phi_{ai} \tag{28}$$

So it is possible to express:

$$\mathbf{Q}^a = \bar{q}\,\phi_{ai}^T \mathbf{G}_{ka}^T \mathbf{S}_{kj} \mathbf{A}_{jj}^{-1} \mathbf{D}_{jk} \mathbf{G}_{ka} \phi_{ai}\,\mathbf{u}_h \tag{29}$$

From Eq. (27), is evident how to perform an aerodynamic gust analysis it is necessary to know the aerodynamic matrix that provides the forces on the aerodynamic elements due to an applied downwash at any other point:

$$\mathbf{Q}_{kj} = \mathbf{S}_{kj}\,\mathbf{A}_{jj}^{-1} \tag{30}$$

which can be expressed in terms of modal coordinates:

$$\mathbf{Q}_{ij}(M,k) = \phi_{ai}^T \mathbf{G}_{ka}^T \mathbf{Q}_{kj} \tag{31}$$

Since extra points cannot affect the gust loading, there are no generalized loading associated with them, so the matrix which provides the generalized loadings in the modal set, $\mathbf{Q}_{hj}$ is obtained adding a null matrix onto the bottom of $\mathbf{Q}_{ij}$.

$$\mathbf{Q}_{hj}(M,k) = \phi_{ai}^T \mathbf{G}_{ka}^T \mathbf{S}_{kj}\,\mathbf{A}_{jj}^{-1} \tag{32}$$

American Institute of Aeronautics and Astronautics

At this point the second term can be expressed as:

$$\mathbf{Q}^e = \bar{q}w_g\mathbf{P}\mathbf{P}(\omega)\boldsymbol{\phi}_{ai}^T\mathbf{G}_{ka}^T\mathbf{S}_{kj}\ \mathbf{A}_{jj}^{-1}\mathbf{w}_j(\omega) \tag{33}$$

The gust downwash matrix, present in Eq. (35), is a function of frequency and the geometry of the aerodynamic model:

$$\mathbf{w}_j(\omega_i) = \cos\gamma_j e^{-i\omega_i(x_j-x_0)/U_\infty} \tag{34}$$

where:

ω_j excitation frequency, or gust frequency
γ_j dihedral angle of the j-th aerodynamic element
x_j x-location of the j-th aerodynamic element in the aerodynamic coordinate system
x_0 reference coordinate for the gust

A.   Correction Method

From Eq.35 the forces acting on the structure due the gust disturbance can be expressed as:

$$\mathbf{F}_a^{DLM} = \bar{q}w_g\mathbf{P}\mathbf{P}(\omega)\boldsymbol{\phi}_{ai}^T\mathbf{G}_{ka}^T\mathbf{S}_{kj}\ \mathbf{A}_{jj}^{-1}\mathbf{w}_j(\omega) \tag{35}$$

Considering the CFD result of full time domain analysis for a sinusoidal gust, once that a periodic response has been reached, it is possible to extract a Fourier transform of the integrated load on the structural grid.

$$\mathbf{F}_a^{CFD}(t) \Rightarrow \Re(\mathbf{F}_a^{CFD}) + i\Im(\mathbf{F}_a^{CFD}) \tag{36}$$

Considering a post multiplying correction approach, if $\mathbf{W}_{jj}^w$ is the correciton matrix that post multiply the *AICs* matrix, it is possible to write:

$$\Re(\mathbf{F}_a^{CFD}) + i\Im(\mathbf{F}_a^{CFD}) = \bar{q}w_g\mathbf{P}\mathbf{P}(\omega)\boldsymbol{\phi}_{ai}^T\mathbf{G}_{ka}^T\mathbf{S}_{kj}\ \mathbf{A}_{jj}^{-1}\{\Re(\mathbf{W}_{jj}^w) + i\Im(\mathbf{W}_{jj}^w)\}\mathbf{w}_j(\omega) \tag{37}$$

In this case the *AICs* matrix is a complex matrix function of the reduced frequency k and of the mach number M:

$$\mathbf{A}_{jj}^{-1}(M,k) = \Re(\mathbf{A}_{jj}^{-1}(M,k)) + i\Im(\mathbf{A}_{jj}^{-1}(M,k)) \tag{38}$$

Acknowledgments

References

[1] E Albano and W. P. Rodden. A Doublet-Lattice Method for Calculating Lift Distributions on Oscillating Surfaces in Subsonic Flows. *AIAA Journal*, 7(2):279–285, 1969.

[2] W. P. Rodden and Paul F. Taylor. Improvements To the Doublet-Lattice Method in MSC Nastran. pages 1–16.

[3] W. P. Rodden, Paul F. Taylor, and Samuel C. McIntosh. Further Refinement of the Subsonic Doublet-Lattice Method, 1998.

[4] Rafael Palacios, H Climent, A Karlsson, and B Winzell. Assessment of strategies for correcting linear unsteady aerodynamics using CFD or experimental results. *International Forum on Aeroelasticity and Structural Dynamics (IFASD)*, 66(172), 2001.

[5] J. P. Giesing, T. P. Kalman, and W. P. Rodden. Correction Factor Techniques for Improving Aerodynamic Prediction Methods. 1976.

[6] Jan Brink-Spalink and J. M. Bruns. Correction of unsteady aerodynamic influence coefficients using experimental or CFD data. In *41st AIAA Conference Atlanta, GA*, 2000.

[7] Ralf Heinrich and N Kroll. Fluid-Structure Coupling for Aerodynamic Analysis and Design A DLR Perspective. *Most*, (January):1–31, 2008.

[8] Stefan Keye. Fluid-Structure-Coupled Analysis of a Transport Aircraft and Comparison to Flight Data. In *39th AIAA Fluid Dynaminamics Conference*, number 22-25 June 2009, pages 1–10, San Antonio, Texas, 2009.

[9]Bernd Stickan, Hans Bleecke, and Silvio Schulze. NASTRAN Based Static CFD-CSM Coupling in FlowSimulator. *Computational Flight Testing Notes on Numerical Fluid Mechanics and Multidisciplinary Design*, 123:223–234, 2013.

[10]Dorian Jones and Ann Gaitonde. Future Fast Methods for Loads Calculations : The FFAST Project. In *Innovation for Sustainable Aviation in a Global Environment proceedings of Aerodays*, pages pp. 110–115.

[11]T. C. S. Rendall and C. B. Allen. Unified fluidstructure interpolation and mesh motion using radial basis functions. *International Journal for Numerical Methods in Engineering*, 74(October 2007):1519–1559, 2008.

[12]T. C. S. Rendall and C. B. Allen. Improved radial basic function fluid-structure coupling via efficient loacalized implementation. *International Journal for Numerical Methods in Engineering*, 78(January):1188–1208, 2009.

[13]MSC Software. MSC Nastran Quick Reference Guide 2014. 2014.

[14]Carmine Valente, Dorian Jones, Ann Gaitonde, J E Cooper, and Yves Lemmens. OPENFSI INTERFACE FOR STRONGLY COUPLED STEADY AND UNSTEADY AEROELASTICITY. In *International Forum on Aeroelasticity and Strucutral Dynamics*, pages 1–16, Saint Petersburg, Russia, 2015.

[15]Ralf Heinrich. Comparison of different approaches for gust modeling in the cfd code tau. pages 1–12.

[16]Gowtham Jeyakumar and Dorian Jones. Aerofoil gust responses in viscous flows using prescribed gust velocities. Technical report, 2013.

[17]C. Wales, Dorian Jones, and A. Gaitonde. Prescribed Velocity Method for Simulation of Aerofoil Gust Responses. *Journal of Aircraft*, pages 1–13, 2014.

[18]Easa. Certification Specifications for Large Aeroplanes CS-25. Technical Report 19 September, 2007.

[19]J. R. Wright and J. E. Cooper. *Introduction to Aircraft Aeroelasticity and Loads.* 2007.